Multilayer model for Hall effect data analysis of semiconductor structures with step-changed conductivity

B. Arnaudov,[1] T. Paskova,[2] S. Evtimova,[1] E. Valcheva,[2] M. Heuken,[3] and B. Monemar[2]
[1]*Faculty of Physics, Sofia University, 5, J. Bourchier Boulevard, 1164 Sofia, Bulgaria*
[2]*Department of Physics and Measurement Technology, Linköping University, S-581 83 Linköping, Sweden*
[3]*Aixtron AG, Kackerstraße 15-17, D-52072 Aachen, Germany*
(Received 22 July 2002; published 16 January 2003)

We present a multilayer model for analysis of Hall effect data of semiconductor structures composed of sublayers with different thicknesses and contacts placed on the top surface. Based on the circuit theory we analyze the contributions of the conductivity of every sublayer and derive general expressions for the conductivity and carrier mobility of a multilayer planar sample. The circuit analysis is performed taking into account the fact that the sample sublayers are partially connected in parallel to each other by series resistances formed in areas lying below the contacts from each upper layer. In order to solve the inverse problem of determining the electrical parameters of one of the sublayers, a procedure for analysis of the Hall effect data is proposed. The model is simplified for a structure composed of two layers with the same type of conductivity, and is used to determine the electrical parameters of GaN films grown on relatively thick GaN buffers.

DOI: 10.1103/PhysRevB.67.045314 PACS number(s): 73.61.Ey, 81.15.Kk

I. INTRODUCTION

Hall effect and conductivity analysis is a widely used method for quantitative evaluation of electrical parameters (carrier concentration n and mobility μ) of semiconductor materials. Being a method that gives average values of the parameters for the studied samples, the main assumption is homogeneity of the electrical properties. However, in real semiconductors, inhomogeneities in the physical properties are often observed. Particularly, epitaxial layers often experience depth inhomogeneities of electron concentration and mobility, either near the surface or at the substrate/layer interface. In order to resolve these peculiarities a multilayer approximation can be used for step changes of the electrical parameters. The simplest approximation, namely, the two-layer model, permits to derive the bulk electrical conductivity and mobility in the presence of an interfacial region.

The two-layer model was firstly suggested by Petritz[1] for a semiconductor sample consisting of a bulk region (with a thickness d_b) and a thin near-surface region (with a thickness d_s, where $d_s \ll d_b$). The model was used to determine the mobility and electron concentration of the near-surface space charge region in a planar sample configuration (large surface area and small thickness). The equivalent circuit used in Ref. 1 was relevant for the sample with laterally placed contacts and a magnetic field perpendicular to the large surface area of the sample. Clearly, when the near-surface layer is very thin, the lateral and top surface placed contacts lead to the same measurement results. Also, the two regions of the sample were considered as interfacially isolated by each other, assuming negligible carrier redistribution between the regions, since it is supposed that the surface conductivity contribution is very small compared to the bulk conductivity. In principal, the electric conduction of a multilayer structure with lateral contacts and interfacially isolated layers can be treated in a similar way as that in a multicarrier homogeneous sample if the electric charge can flow between layers at the side of the sample just to the perfectly conducting contacts.[2,3] The layers in such structures are called completely connected in parallel. The effect of the carrier transfer between the layers becomes important at high magnetic fields and/or in heterostructures with high-mobility two-dimensional electron gas at the heterointerface[4] and cannot be neglected, however, at low magnetic fields typically used in Hall effect measurements, the distinction between two-band and two-layer models is not important.[3,5]

The two-layer approximation based on the two-band (i.e., two-carrier) conductivity interpretation was used for modeling a parallel conduction path in some specific GaAs/AlGaAs heterostructures[6,7] and in GaInAs/AlInAs heterostructures under hydrostatic pressure[8] and was found to provide a good description of the observed peculiarities. In Ref. 6 the parallel conduction between the interface channel and the undepleted AlGaAs layer in a two-terminal sample with top surface contacts was analyzed using an equivalent circuit with three additional resistances: contact resistance to the AlGaAs layer, interlayer resistance and resistance between the interface channel and the contact. In four-terminal samples for Hall effect measurements[7] the influence of the resistances between the layers and the contacts was eliminated and the electric field in the two layers was assumed to be the same. The two-layer model for a direct problem analysis of Hall effect data of GaAs modulation doped field-effect transistors was developed by Look.[9,10] It was shown that in some cases of specific defect level distribution the two-layer approximation was sufficient for determination of two-dimensional electron gas concentration and mobility, but it was pointed out that difference between two-band and two-layer problems should be considered in the general case.

Recently, the two-layer model was used for analysis of GaN layers heteroepitaxially grown on sapphire with a highly defective substrate/layer interface region, found to have degenerate electrical behavior.[11–13] The model was applied to samples with contacts placed on the top surface and its validity was ensured since the interface sublayer is ex-

0163-1829/2003/67(4)/045314(10)/$20.00 ©2003 The American Physical Society

tremely thin (200-nm thickness) and the contribution of the interface region conductivity to the bulk conductivity is rather small. The top surface positions of the contacts in such a case are not expected to affect the calculated results, although the original model[1] assumes laterally connected regions of the sample. However, in some cases, for instance in Si-doped metalorganic chemical vapor deposited (MOCVD) GaN layers,[14] the two-layer analysis of the transport properties could not explain the temperature behavior of the electrical parameters because of the fact that the standard two-band interpretation was a considerable oversimplification of the real situation and requires a consideration of impurity band conductivity contribution. Additionally, in semiconductor samples composed of sublayers with comparable thicknesses, particularly in homoepitaxial layers grown on relatively thick buffers, the contribution of the underlying sublayer to the whole sample conductivity may be significantly higher. A similar situation also exists in unipolar structures like vertical n^+n structures for Schottky barrier device applications. These cases do not fall into the framework of validity of the two-layer model.

In this work, we present a multilayer model for analysis of Hall effect data of samples with top surface contacts and different thicknesses of the sublayers. For this, a detailed balance of the contribution of each sublayer to the whole sample conductivity and Hall mobility has been considered. A circuit analysis is performed considering the fact that in the general case the sublayers are partially connected in parallel to each other by series resistances formed in areas lying below the contacts from each upper layer. Correction factors, which reduce the contribution of the underlying layers to the measured total sample conductivity, are obtained from the equations relevant to the equivalent circuit. In order to solve the inverse problem of determining the electrical parameters of one of the sublayers, a procedure for analysis of the Hall effect data is proposed.

The model was then simplified for a two-layer structure and applied for calculation of the electron concentration and mobility of thick GaN layers grown by hydride vapor phase epitaxy (HVPE) on sapphire with MOCVD-GaN templates. The electrical parameters of the templates have been independently measured. Different experimental situations were chosen to provide a quantitative comparison with the theory and to demonstrate specific approximations of the developed model. The treatment we suggest is more general and can be regarded as an extension of the analysis based on the conventional two-layer model.

The paper is organized as follows. In Sec. II we derive general expressions for the conductivity and carrier mobility in multilayer planar samples in the presence of a longitudinal electric field and a magnetic field applied perpendicular to the surface area. Section II A presents the general case of partially connected layers with surface placed contacts. Based on the circuit theory we analyze the contribution of the conductivity and mobility of the sublayers to the measured electrical parameters of the whole sample and derive correction factors. Section II B is limited to the case of completely connected layers with laterally placed contacts. In Sec. III we solve the inverse problem in a particular case of a two-layer structure, i.e., we estimate the electrical parameters of the upper sublayer of interest, knowing the parameters of the entire structure and of the underlying sublayer. Experimental results and analytical estimation of correction factors and electrical parameters of the sublayers are presented in Sec. IV, analyzing different approximations of the suggested model. In Sec. V the main conclusions of the paper are summarized.

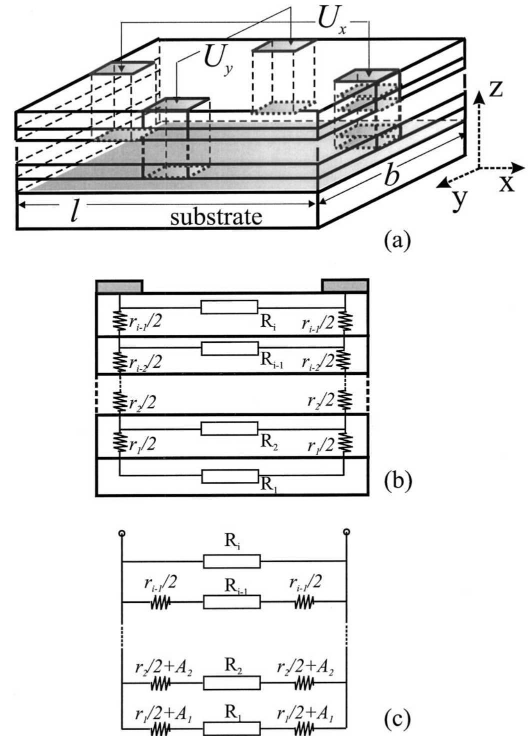

FIG. 1. (a) Schematic drawing of a multilayer structure with top surface contacts. Equivalent circuits for Hall effect measurements of real series type (b) and transformed parallel type (c). The circuits present the part for the applied voltage contacts. The various parameters are defined in the text.

II. MULTILAYER MODEL

We assume that the i-fold multilayer planar sample analyzed here is oriented in the xy plane. Both bar-shaped and van der Pauw configuration samples will be considered. The total thickness of the sample is $d=\Sigma_i d_i$, where d_i is the thickness of the ith layer, and all the layers comprising the sample structure are parallel to the xy plane [Fig. 1(a)]. The applied electric field is parallel to the x axis (E_x) and the applied magnetic field is longitudinal to the z axis (B_z). Thus, the electric field (E_y) induced by Hall effect, is normal to E_x and parallel to the y axis. We also neglect the carrier redistribution between the layers assuming that the layers are interfacially isolated from each other and connected by both current and Hall voltage contacts in parallel. The total sample current I_x due to the applied electric field E_x is a sum of the partial currents of every ith layer:

$$I_x = \sum_i I_{x,i} \tag{1}$$

and the sum of the partial currents in the y direction $I_{y,i}$, giving the total current I_y, is zero:[8]

$$I_y=\sum_i I_{y,i}=0. \tag{2}$$

We point out that in Hall effect measurements the real conductivity and mobility cannot be measured directly. Indeed we measure either the ratio between the current and the applied voltage for calculation of the conductivity or the ratio between the open circuit Hall effect voltage and the applied voltage (and divide by the magnetic induction B_z) for the mobility calculation. Afterwards, we transform the measured ratios into conductivity and mobility units. Thus, for the ith layer the following relations are obtained:

$$\frac{I_{x,i}}{U_{x,i}}=\frac{b}{l}\sigma_i d_i, \tag{3}$$

$$\frac{U_{y,i}}{U_{x,i}B_z}=\frac{b}{l}\mu_i. \tag{4}$$

Here b and l are the width and length of the bar sample, respectively. For nearly square sample the value b/l is close to unity. In case of van der Pauw configuration, the ratio b/l is determined numerically from the electrical non-symmetry of the sample by van der Pauw function.[15] In Eqs. (3) and (4) $U_{x,i}$ is the applied voltage to the ith layer of the sample, $U_{y,i}$ is the voltage induced in ith layer by the Hall effect, σ_i is the conductivity and μ_i is the low magnetic field Hall mobility of the ith layer. The potential drop values $U_{x,i}$ and $U_{y,i}$ correspond to the electric field components ($E_{x,i}=U_{x,i}/l$, $E_{y,i}=U_{y,i}/b$). It is seen that the partial current $I_{x,i}$ in the ith sublayer of the sample is proportional to both the applied voltage $U_{x,i}$ and the sheet conductivity $\sigma_i d_i$.

Further in order to solve the inverse problem, i.e., to estimate the electrical parameters of one or more of the sublayers of interest knowing the parameters of the entire structure and of the other sublayers, we have to express the sheet conductivity and mobility of the whole sample via measured ratios by analogy with Eqs. (3) and (4):

$$\frac{I_x}{U_x}=\frac{b}{l}\sigma^* d, \tag{5}$$

$$\frac{U_y}{U_x B_z}=\frac{b}{l}\mu^*. \tag{6}$$

We use an effective sheet conductivity ($\sigma^* d$) and Hall mobility (μ^*) of the whole sample, which correspond to the measured voltages U_x, U_y and the current I_x, since the values of the real sheet conductivity and Hall mobility might differ. Here, the potential drop values U_x and U_y are also used, instead of the corresponding electric field components ($E_x=U_x/l$, $E_y=U_y/b$).

Further, replacing Eqs. (3)–(6) into Eqs. (1) and (2) we express the effective sheet conductivity and mobility of the entire sample [left-hand sides in Eqs. (1) and (2)] and the corresponding sum of all i layers [right-hand sides in Eqs. (1) and (2)] via measurable parameters. Taking into account that the dimensions l and b do not vary in the different sublayers, we obtain the following general equations for Hall effect data analysis:

$$\sigma^* d=\frac{1}{U_x}\sum_i U_{x,i}\sigma_i d_i, \tag{7}$$

$$\mu^*\sigma^* d=\frac{1}{U_x U_y}\sum_i U_{x,i}U_{y,i}\mu_i\sigma_i d_i. \tag{8}$$

We note that Eqs. (7) and (8) are generally valid for any multilayer semiconductor system upon the following assumptions: (i) uniaxial inhomogeneity with a step change of the conductivity and (ii) negligible carrier redistribution between the sublayers of the system. In the next sections we use Eqs. (7) and (8) for analysis of Hall effect data for samples with different contact configurations and discuss the applicability of the suggested model for the inverse problem solution.

A. Partially connected layers with top surface contacts

We consider a multilayer sample with contacts placed on the top surface [Fig. 1(a)]. This consideration is especially important when any of the thicknesses of the sublayers cannot be neglected and the area of the contacts (s) is significantly smaller than the total area of the sample.

The equivalent circuit of a multilayer system for the part related to the applied voltage U_x is shown in Fig. 1(b). The longitudinal resistances of the ith layer along the x direction, i.e., sample dimension l, are R_i^x (labeled R_i in the figure). The corresponding transverse (along the y direction, i.e., sample dimension b) resistances in the part related to the Hall effect induced voltage U_y, (not shown in the figure) are R_i^y. Their values are given by the definition of bulk resistance

$$R_i^x=\frac{1}{\sigma_i}\frac{l}{bd_i},\quad R_i^y=\frac{1}{\sigma_i}\frac{b}{ld_i}. \tag{9}$$

In such a case, hereafter called case of partially connected layers, every ith layer of the sample is not directly connected to the contacts, in fact it is connected in parallel to the other sublayers through series resistances r_i^x [where $r_i^x=(1/\sigma_{i+1})\times(2d_{i+1}/s)$] in the circuit of the applied voltage. The series resistances r_i^x are formed in areas lying below the contacts from each upper layer since the ratio d_i/σ_i is not always negligible. Indeed, when the contacts are placed on the top surface, the bulk resistances connecting every underlying layer will include a contribution of the resistances of all upper layers [labeled $A_1,\ldots,A_{i-2}$ in Fig. 1(c)]. The series resistances connecting the top layer to the contacts will be equal to zero. The situation corresponds to a series type of equivalent circuit for the resistances r_i^x. Based on the circuit theory such a series type equivalent circuit can be transformed into a parallel type equivalent circuit [Fig. 1(c)]. Further on we will use the parallel equivalent circuit which is more convenient for analytical calculations. In the figure, r_i^x

denotes the whole series resistance of the ith sublayer, which is actually distributed in two nearly equal parts below the two current contacts. The same consideration can be made for the series resistances r_i^y for the respective circuit related to the two Hall voltage contacts (not shown).

We note that the four-point configuration used in Hall effect and conductivity measurements eliminates the influence of the contact resistances, since the voltages determined by Hall effect and conductivity are measured on a contact pair, which is separated from the pair of current contacts. When the contacts are placed on the top surface, the contact resistances are the same for all the sublayers, and we do not account for them in the equivalent circuits shown in Fig. 1.

Using circuit analysis, we obtain the following expressions for the voltages $U_{x,i}$ applied to every ith sublayer

$$U_{x,i}=U_x\frac{R_i^x}{R_i^x+r_i^x}, \tag{10}$$

and for the voltages induced by Hall effect in every sublayer

$$U_{y,i}=U_y\frac{R_i^y}{R_i^y+r_i^y}. \tag{11}$$

Substituting the values of $U_{x,i}$ and $U_{y,i}$ derived by Eqs. (10) and (11) into Eqs. (7) and (8) we obtain expressions for Hall effect data analysis in a multilayer system with partially connected sublayers

$$\sigma^* d=\sum_i \sigma_i d_i\frac{R_i^x}{R_i^x+r_i^x}, \tag{12}$$

$$\mu^*\sigma^* d=\sum_i \mu_i\sigma_i d_i\frac{R_i^x}{R_i^x+r_i^x}\frac{R_i^y}{R_i^y+r_i^y}. \tag{13}$$

Equations (12) and (13) show that for structures with top surface contacts the current distribution between the sublayers depends on both the sheet conductivity (and consequently on the mobility) of the ith sublayer and on the series resistances connecting the layers in parallel.

The terms in Eqs. (10) and (11) determined by the ratios of the respective resistances

$$t_i^x=\frac{R_i^x}{R_i^x+r_i^x},\quad t_i^y=\frac{R_i^y}{R_i^y+r_i^y} \tag{14}$$

actually reduce the contribution of the ith layer to the measured sheet conductivity and mobility of the whole sample. As one can see, these factors are either lower than unity or equal to unity when the series resistances r_i^x and r_i^y can be ignored, and they can be considered as correction factors, t_i^x for the applied voltages $U_{x,i}$, and t_i^y for the Hall effect induced voltages $U_{y,i}$ for each ith sublayer.

Analyzing Eqs. (11) and (12) it is clear that in the inverse problem solution, if the values of the sheet conductivity and mobility of the ith layer are used without being corrected by the terms t_i^x and t_i^y, then their contribution to the measured total sample conductivity and mobility might be overestimated. This will result in an underestimated conductivity and mobility of the sublayers of interest. In some cases when the underlying sublayer has high enough conductivity and is relatively thick, even an artifact of its negative contribution to the total sample conductivity can be observed. The only way to circumvent this problem is to use Eqs. (7) and (8) accounting for the suggested correction factors t_i^x and t_i^y.

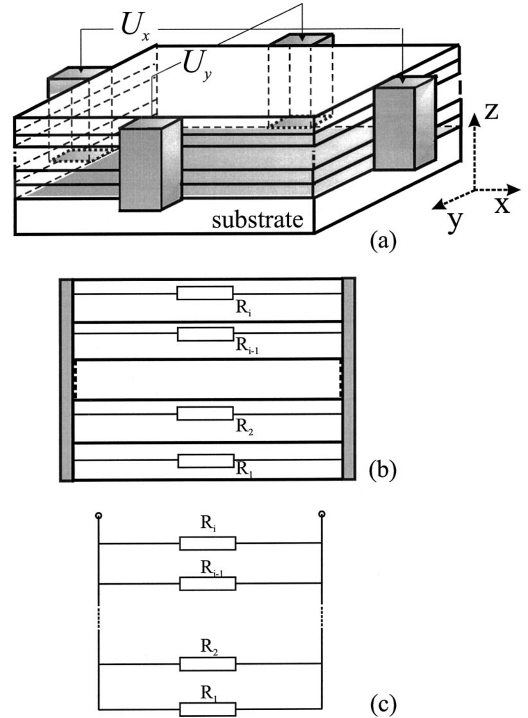

FIG. 2. (a) Schematic drawing of a multilayer structure with lateral contacts and (b), (c) equivalent circuits for Hall effect measurements.

The values of t_i^x and t_i^y cannot be calculated precisely in reality but their influence can be, in principle, accounted for by iteration procedures. Since in the van der Pauw configuration the ratio b/l is typically close to unity we assume $R_i^x \approx R_i^y$ and $r_i^x \approx r_i^y$. Thus in order to simplify our further calculations we use equal correction factors for both applied voltage and Hall effect induced voltage for each ith layer, $t_i^x=t_i^y=t_i$. In the case of bar-shaped sample the term t_i represents the mean value of the correction factors t_i^x and t_i^y, $t_i\equiv(t_i^x t_i^y)^{1/2}$.

B. Completely connected layers with lateral contacts

Now we consider a multilayer sample with laterally placed contacts [Figs. 2(a), and 2(b)]. This case is realized if every sublayer of the structure is directly connected in parallel to the contacts independently of the other sublayers. Hereafter we call this the case of completely connected layers.

The equivalent circuit of such a system for the part concerning the applied voltage U_x is shown in Fig. 2(c). This circuit is not too different from the equivalent circuit shown in Fig. 1(c), in fact it can be obtained from the previous circuit assuming that the series resistances are neglected, r_i^x

$=r_i^y=0$. It is clear that the voltages $U_{x,i}$ applied to every ith layer in the x direction are similar and equal to the voltage drop U_x supplied to the whole sample

$$U_{xi}=U_x. \tag{15}$$

Such an identity is also valid for the Hall effect induced voltages $U_{y,i}$ and U_y:

$$U_{y,i}=U_y. \tag{16}$$

Using Eqs. (15) and (16), we express the real sheet conductivity and mobility of the whole sample via the parameters of the sublayers as follows:

$$\sigma d=\sum_i \sigma_i d_i, \tag{17}$$

$$\mu\sigma d=\sum_i \mu_i\sigma_i d_i. \tag{18}$$

Equations (17) and (18) reflect the fact that in the case of completely connected layers the distribution of partial currents $I_{x,i}$ in every ith layer [see Eqs. (1) and (2)] is determined only by the partial sheet conductivity $\sigma_i d_i$ and mobility μ_i of the same layer. This situation is realistic because the applied electric field E_x, as well as that induced by the Hall electric field E_y, do not vary in the different layers and they can be derived as a constant in front of Eqs. (7) and (8) and thus instead of currents, the current densities can be used.

It is worth nothing that Eqs. (16) and (17) derived for a multilayer system with completely connected sublayers coincide with the expressions for multicarrier transport,[16] which are obtained by summarizing the longitudinal (parallel to the applied electric field E_x) net conductivity tensor components $\sigma_{xx,i}$, as well as, transverse (normal to E_y) components $\sigma_{xy,i}$, contributed by each ith carrier. The fundamental equations for multicarrier transport are based on the fact that the partial currents contributed by all i types of carriers take place in the entire volume of the sample, which is common for all carriers. In this case the electric field components for every ith type of carriers are similar and equal to the voltage drop supplied to the whole sample U_x divided by l, or to the Hall effect induced voltage U_y, divided by b, respectively. Therefore, one always summarizes only the partial current densities.

In spite of the fact that in the multilayer system the partial currents in the different layers are spatially separated, if the voltages applied to each sublayer are the same (and, respectively, the voltages induced by Hall effect are also equal), we obtain that the electric fields in all sublayers are equal. Thus, the equations for multicarrier electron transport can be applied to the multilayer system if Eqs. (15) and (16) are satisfied, i.e., any difference between the values of $U_{x,i}$ or $U_{y,i}$, respectively, can be ignored. This is valid if the lateral contacts connecting every ith layer in parallel are of low or equal contact resistance. If the contact resistances of one of the sublayers are higher than those of the rest sublayers, this layer cannot be treated as completely connected anymore. Actually, it becomes partially connected and the circuit should be transformed to a partially connected type similar to that discussed in the previous section with the only difference that here in the equivalent circuit, we should consider contact resistances instead of the bulk resistances [as shown in Fig. 1(c)].

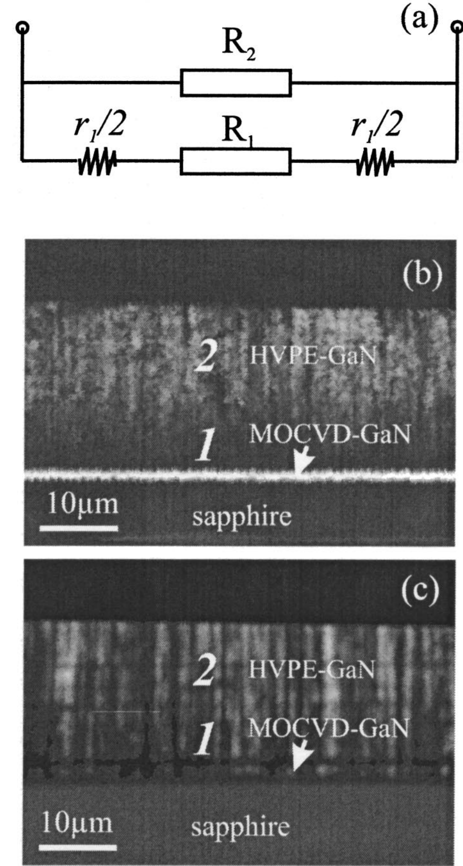

FIG. 3. (a) Equivalent circuit for Hall effect measurements for a two-layer structure. Panchromatic CL images of cross sections of two two-layer structures with (b) strong emission contrast indicating a significant difference in their carrier concentrations and (c) with similar emission intensity indicating comparable carrier concentrations of the sublayers.

III. PARTIALLY CONNECTED TWO-LAYER STRUCTURE

In this section we consider a two-layer structure with top surface contacts aiming to simplify the above discussed model for the inverse problem solution, hereafter called extended two-layer model. For this reason we rewrite Eqs. (12) and (13) taking into account the correction factors

$$\sigma^* d=\sigma_1 d_1 t_1+\sigma_2 d_2 t_2, \tag{19}$$

$$\mu^*\sigma^* d=\mu_1\sigma_1 d_1 t_1^2+\mu_2\sigma_2 d_2 t_2^2. \tag{20}$$

For simplicity we define that the first layer is underlying and the contacts are placed on the second layer. In this case we can neglect the series resistance connecting the upper layer, $t_2=1$ [Fig. 3(a)] and obtain a case of partially connected underlying layer. We consider also that the parameters of the underlying layer have been independently measured, which

is chronologically possible. An example of the inverse problem for the two-layer structure is calculation of the parameters of the next upper layer from the measured effective conductivity and mobility of the whole sample. From Eqs. (19) and (20) we obtain

$$\sigma_2 d_2 = \sigma^* d - \sigma_1 d_1 t_1, \tag{21}$$

$$\mu_2 \sigma_2 d_2 = \mu^* \sigma^* d - \mu_1 \sigma_1 d_1 t_1^2. \tag{22}$$

In this simple case the correction factor t_1 is given by the expression (assuming $b/l \approx 1$)

$$t_1 = \frac{1}{1 + (\sigma_1/\sigma_2)(2d_1 d_2/s)}. \tag{23}$$

The values of t_1, n_2, and μ_2 can be estimated from Eqs. (21)–(23) by a single-step numerical iteration. We first estimate the uncorrected value of the conductivity of the upper layer σ_2^0 from Eq. (21), initially assuming $t_1 = 1$. This value σ_2^0 can be substituted in Eq. (23) instead of σ_2 and we obtain a first order approximation of t_1. Afterwards, we replace this value of t_1 in Eqs. (21) and (22) and estimate the first order approximation of the conductivity σ_2 and mobility μ_2 of the layer of interest.

We note that the use of σ_2^0 for a zero-approximation calculation is not always possible. When the measured values of the sheet conductivity and mobility of the whole sample are lower than the independently measured parameters of the underlying layer $\mu^* \sigma^* d < \mu_1 \sigma_1 d_1$, the iterative process cannot be applied and it is necessary to solve the system of Eqs. (21) and (22) by numerical methods.

Using Eqs. (21) and (22) for a two-layer structure and having in mind the relations between Hall mobility μ_i and the sheet carrier concentration n_i^{sh} for the ith layer on one hand, and between the effective conductivity $\sigma^* d$ and the effective sheet carrier concentration $n^{\mathrm{sh}*}$ for the whole sample on the other hand,

$$n_i^{\mathrm{sh}} = n_i d_i \equiv \frac{\sigma_i d}{e \mu_i}, \quad n^{\mathrm{sh}*} = n^* d \equiv \frac{\sigma^* d}{e \mu^*}, \tag{24}$$

we obtain the following expressions for the electron concentration n_2 and mobility μ_2 versus the correction factor t_1:

$$n_2 = \frac{1}{d_2} \frac{(\mu^* n^* d - \mu_1 n_1 d_1 t_1)^2}{\mu^{*2} n^* d - \mu_1^2 n_1 d_1 t_1^2}, \tag{25}$$

$$\mu_2 = \frac{\mu^{*2} n^* d - \mu_1^2 n_1 d_1 t_1^2}{\mu^* n^* d - \mu_1 n_1 d_1 t_1}. \tag{26}$$

The system of Eqs. (25) and (26) can be solved numerically by varying the parameter t_1 in the range of its physical meaning between 0 and 1, and the dependencies of electron concentration n_2 and mobility μ_2 of the upper layer of interest on the correction factor t_1 can be obtained for fixed values of the measured parameters n_1 and μ_1, and n^* and μ^*.

We point out that the system of Eqs. (25) and (26) might be solved analytically only if one more relation can be found for the correction factor t_1. The latter is possible for some particular cases (see Sec. IV B).

IV. EXPERIMENTAL RESULTS AND DISCUSSION

A. Experimental details

We studied GaN structures grown on *c*-plane sapphire. In order to improve the crystal quality of the thick HVPE grown GaN we used MOCVD-GaN templates.[17,18] The first layers of the structures were grown in a planetary type MOCVD reactor in the Aixtron application laboratory at high growth temperature of about 1170 °C. Two types of MOCVD templates with thicknesses in the range of 2–2.5 μm, intentionally doped with Si with a free carrier concentration in the range of 10^{18} cm^{-3} and intentionally undoped GaN layers with a free carrier concentration in the range of 10^{17} cm^{-3} were used. The second GaN layers of the structures were grown in a conventional horizontal type HVPE system at 1090 °C. We have also analyzed layers grown without a buffer with highly defective interface columnar region previously found to be highly conducting.[13,19] The thicknesses of the HVPE-GaN layers were in the range of 10–45 μm.

Hall measurements were carried out at room temperature on nearly square samples with alloyed In+Ga Ohmic contacts using the van der Pauw method. We have measured samples consisting only of the MOCVD-GaN templates and the entire structures after the HVPE growth of the second layers. All samples studied show *n*-type conductivity. We calculate the concentration of free electrons and the mobility using the extended two-layer model. Several experimental situations were chosen to demonstrate the different approximations of the presented model. The calculated free carrier concentrations and mobilities for five representative samples are summarized in Table I. Schottky contacts were deposited by magnetron sputtering of Pt for independent measurement of the carrier concentration by capacitance-voltage (C-V) technique.

B. Structures with dominating sheet conductivity of the underlying layer

As a representative sample for this case we consider sample No. 1 consisting of a 2.5-μm-thick Si-doped MOCVD-GaN template and undoped 21.5-μm-thick HVPE-GaN layer. A panchromatic CL image of a cross section of such a structure is shown in Fig. 3(b). The image reveals a strong emission contrast of the two layers related to different doping level and also illustrates a step change of the conductivity. Hall effect measured values of electron concentration and mobility of the template as well as of the entire structure are listed in Table I. It is seen that the sheet conductivity of the underlying layer is higher than that of the whole sample, i.e., $\sigma_1 d_1 > \sigma^* d$, and also the following inequality is seen: $\mu_1 \sigma_1 d_1 > \mu^* \sigma^* d$. In such a case, a numerical solution of Eqs. (25) and (26) by variation of t_1 is the only possible way to determine the parameters of the upper layer. In the range of varying the correction factor ($0 < t_1 < 1$), the mobility μ_2 has a maximum at a certain value t_1^* [Fig. 4(a), curve 1]

TABLE I. Electrical parameters measured directly by Hall effect measurements of both the templates and the whole structures, as well as calculated electrical parameters of the second layer of interest for five GaN structures representing different experimental cases.

Sample No.	Sample thicknesses d_1/d_2 (μm/μm)	Directly measured template n_1 (cm^{-3})	Directly measured template μ_1 (cm^2/V s)	Directly measured whole structure n^* (cm^{-3})	Directly measured whole structure μ^* (cm^2/V s)	Correction factor t_1	Calculated for the second layer according to Eqs. (25), (26) n_2 (cm^{-3})	Calculated for the second layer according to Eqs. (25), (26) μ_2 (cm^2/V s)	Calculated for the second layer according to Ref. 1 n_2 (cm^{-3})	Calculated for the second layer according to Ref. 1 μ_2 (cm^2/V s)
1	2.5/21.5	1.35×10^{18}	286	2.4×10^{17}	217	0.45	1.9×10^{17}	265	<0	<0
							1.8×10^{17}[a]	260[a]		
2	2/18.5	1.8×10^{18}	250	2.3×10^{17}	270	0.86	9×10^{16}	365	6.2×10^{16}	320
						0.74[b]	7.4×10^{16}[b]	355[b]		
3	2.5/7.8	2×10^{17}	78	3.6×10^{17}	516	0.96	3.1×10^{16}	627	3×10^{16}	629
Ref. 12	0.2/20	3.9×10^{19}	55	1.7×10^{17}	633	0.98	1.1×10^{17}	778	1.1×10^{17}	781
4	4/40	2.7×10^{19}[c]	53[c]	1.26×10^{19}	66	0.1[d]	4.5×10^{17}	350	1.24×10^{19}	66

[a]According to graphs 1 [Figs. 4(a) and 4(b)].
[b]According to single step iteration.
[c]Values measured by calibration procedures of RS and CL spectra.
[d]Correction factor for the second partially connected layer t_2.

while the carrier concentration of the investigated layer n_2 decreases monotonically in the whole range with increase of the correction factor t_1 [Fig. 4(b), curve 1]. It is important to clarify that the terms in the left-hand sides of Eqs. (21) and (22) could become negative at the highest values of the correction factor ($t_1 \approx 1$) due to the fact that the sheet conductivity of the underlying layer dominates over the whole sample sheet conductivity. The range of the values, where the corrected electron concentration n_2 shows an increase [see Fig. 4(b)], should be ruled out in the variation procedure since the whole sample sheet conductivity becomes negative and does not have a physical meaning ($\sigma_1 d_1 t_1 > \sigma^* d$).

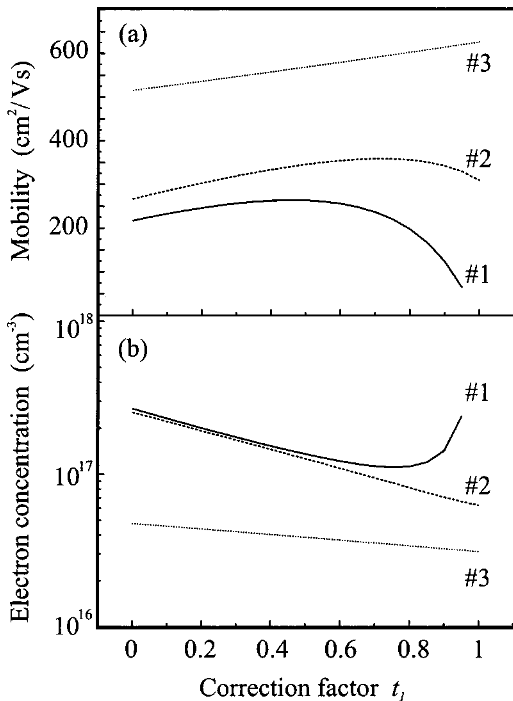

FIG. 4. Dependencies of electron mobility (a) and concentration (b) on the correction factor t_1 for sample Nos. 1, 2, and 3 (as indicated in Table I) illustrating different cases of application of the suggested model.

The existence of a maximum (if such exists) in the dependence of the mobility μ_2 on the correction factor ensures one more relation. Coming back to Eq. (26) we can equalize the derivative of $\mu_2(t_1)$ to zero. This leads to the following equation for the value t_1^*:

$$t_1^* = \frac{\mu^* n^* d}{\mu_1 n_1 d_1}\left[1 - \left(1 - \frac{n_1 d_1}{n^* d}\right)^{1/2}\right]. \tag{27}$$

Note that it is necessary to assume $n^* d > n_1 d_1$ in order to obtain a real solution of the quadratic equation, but this is a reasonable assumption since the whole sample sheet concentration $n^* d$ is a sum of the partial sheet concentrations of the sublayers. Equation (27) actually gives us the needed additional expression for the correction factor t_1^* and ensures an analytical solution of the inverse problem. Using the calculated value $t_1^* = 0.45$ we are able to estimate the electron concentration n_2 and the mobility μ_2 of the upper layer from Eqs. (25) and (26). The obtained values are shown in Table I. The analytically determined values of n_2 and μ_2 coincide with the values of the mobility estimated by variation procedure [maximum mobility in Fig. 4(a)] and the respective electron concentration (for the same t_1) from Fig. 4(b) within the accuracy of both estimations. The electron concentration ($n_2 = 1.9\times10^{17}$ cm^{-3}) of the upper layer calculated according to the extended two-layer model is lower and the mobility value ($\mu_2 = 265$ cm^2/V s) is higher than the measured whole sample effective concentration and mobility ($n^* = 2.4\times10^{17}$ cm^{-3}, $\mu^* = 217$ cm^2/V s). This result is reasonable, having in mind that the overgrown layer is intentionally undoped. In addition, independently performed C-V measurement of the upper layer of the structure (with both contacts placed on the top surface) yields a value of the

electron concentration of 2×10^{17} cm^{-3}, which is very close to the value determined by the extended two-layer model and thus, confirms its relevance.

Here we note that the extended two-layer model, accounting for the correction factor, is the only way to solve the inverse problem for the two-layer semiconductor structure with top surface placed contacts in the case of dominating sheet conductivity of the underlying layer. Since such n^+n semiconductor structure is very realistic and common, the necessity of the model suggested here is clear.

It should be also mentioned that the above procedure allows a treatment of a multilayer structure as well. For this we proceed step by step assuming the whole structure as a quasi-two-layer structure, consisting of the lowest (or the top) layer with independently known electrical parameters as the first layer, and the rest layers all together as the second package layer. Upon this assumption we calculate the parameters of the package layer. After that, the package layer can be consequently analyzed in a similar way as a quasi-two-layer structure and using additional independently known parameters of one of the sublayers, one can repeat the calculation for the next layers, etc.

C. Structures with lower and comparable sheet conductivity of the underlying layer

A sample demonstrating this case (No. 2, see Table I) is also consisting of a 2-μm-thick Si-doped MOCVD-GaN template and undoped 18.5-μm-thick HVPE-GaN layer. The measured sheet conductivity of the template $\sigma_1 d_1$ is lower than that of the whole sample $\sigma_1 d_1 \leqslant \sigma^* d^*$. In order to estimate the electron concentration n_2 and mobility μ_2 of the upper layer we proceed in the same way as in Sec. IV B.

The respective variation of μ_2 and n_2 versus the correction factor t_1 calculated following Eqs. (25) and (26) are shown in Figs. 4(a) and 4(b), (curves 2). For this approximation, the correction factor t_1 can be varied in the whole range between 0 and 1 since the required inequality $\sigma_1 d_1 t_1 < \sigma^* d$ is always satisfied independently of t_1. The two dependencies exhibit the same character as those for the sample No. 1, although the maximum in the mobility dependence is shifted to higher value of the correction factor t_1. The estimated value of the t_1 according to Eq. (27) gives a value of 0.86 and thus showing that the correction needed in this case is smaller.

The electron concentration n_2 and mobility μ_2 of the upper layer estimated from Eqs. (25) and (26) are shown in Table I. The values of n_2 and μ_2 estimated by the extended two-layer model are compared to the values obtained by to the conventional two-layer model,[1] also listed in Table I. It is seen that the suggested model gives higher values of both carrier concentration and mobility of the upper layer compared to those estimated by the two-layer model. The difference in the mobility values is more essential: $\mu_2 = 365$ cm^2/V s compared to $\mu_2 = 320$ cm^2/V s, while the difference in the electron concentration is rather small, $n_2 = 9\times10^{16}$ cm^{-3} according to the extended two-layer model versus $n_2 = 6.2\times10^{16}$ cm^{-3} according to the two-layer model. The latter leads to a change of the compensation ratio as well. This explains the unexpected high value of the compensation based on the directly measured results, which was in contradiction with the results obtained from luminescence investigation of these samples.[20,21] This can be considered as an indication of a reliability of the suggested model.

We mention that in this case one can also use the proposed in Sec. III iteration process to estimate the correction factor t_1. The single-step iteration gives comparable values of n_2 and μ_2, (see Table I) within an accuracy of about 20%, which is in a good agreement with analytically determined values. This is a simple and effective approach to estimate the electrical parameters of a two-layer structure, which can be used when $\sigma_1 d_1 < \sigma^* d$ and $\mu_1 \sigma_1 d_1 < \mu^* \sigma^* d$.

D. Structures with negligible sheet conductivity of the underlying layer

Sample No. 3 presents a structure composed of a HVPE-GaN layer grown on an intentionally undoped template. Figure 3(c) shows a panchromatic CL image of a cross section of such a structure. The emission intensities of the two layers do not differ essentially and correspond to comparable doping levels of the template and the overgrown layer. The Hall effect measured values of electron concentration of the template and of the entire structure (see Table I) are comparable. Since the mobility of the template is much lower than the measured mobility of the entire structure ($\mu^* = 515$ cm^2/V s and $\mu_1 = 78$ cm^2/V s, respectively), the sheet conductivity of the template becomes negligible $\sigma_1 d_1 \ll \sigma^* d$.

The plot of carrier mobility of the upper layer μ_2 shows a monotonic increase while the electron concentration n_2 shows a decrease with increasing the correction factor t_1. In fact, $\mu_2(t_1)$ obtains a degenerate maximum at the highest limit of the physical meaning of the correction factor $t_1 = 1$. The correction factor t_1 calculated from Eq. (27) is close to unity, $t_1^* = 0.96$.

Another case of negligible sheet conductivity of the underlying sublayer is illustrated by analyzing a sample with highly degenerate ($\sigma_1 > \sigma^*$) and extremely thin ($d_1 \ll d$) interface sublayer reported in Ref. 12. The measured parameters for this sample are also listed in Table I. It is seen that there is a strong inequality of the sheet conductivities, $\sigma_1 d_1 \ll \sigma^* d$. This allows us to neglect the series resistances r_1^x and r_1^y [according to Eq. (14)]. Thus, the underlying thin sublayer could be considered completely connected to the contacts. The equivalent circuit for this structure is similar to that shown in Fig. 2(c).

The calculated value of t_1 according to the extended two-layer model for these particular parameters appears to be very close to unity ($t_1 = 0.98$), i.e., the correction factor here can be neglected. Thus, we obtain values for the mobility μ_2 and carrier concentration n_2 that are very close to the results obtained in Ref. 12 following the two-layer model. This is not surprising keeping in mind that the two-layer model is developed exactly for such boundary conditions.[1] The good agreement between the results obtained by both approaches is indicative of their relevance. Note, that the two samples

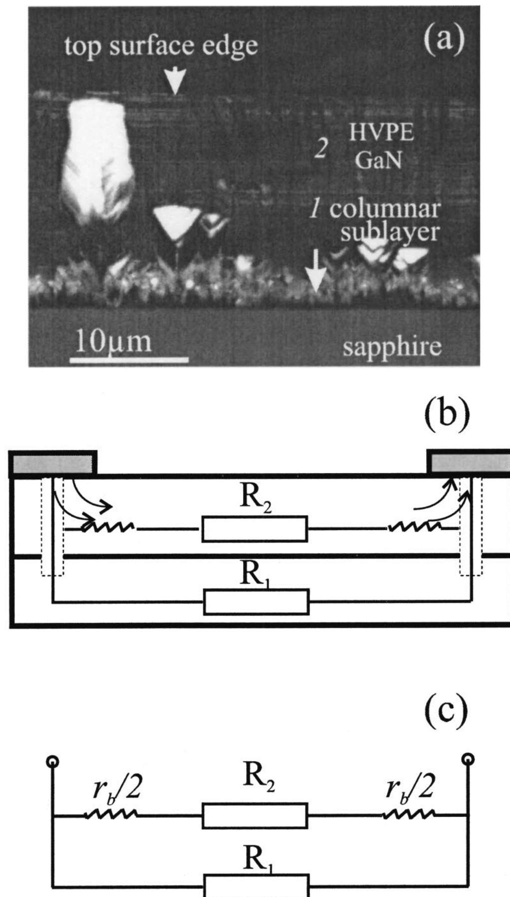

FIG. 5. (a) Panchromatic image of cross section of thick GaN film grown directly on sapphire showing a quasicontinuous columnar interface layer (considered as sublayer 1) and a column protruding to the top surface. (b) A schematic illustration of possible current paths and (c) equivalent circuit for a structure with bypassing the underlying layer through conductive columns. (Dashed rectangulars present the columns).

considered in this section are very different in a general sense but they appear in the same group and require the same analytical treatment.

E. Structures with bypassing conductivity of the underlying layer

This specific case does not fall into the above discussed groups but it can be reasonably analyzed by the suggested model and is included here to show an additional application of the model. We consider a sample (No. 4 in Table I) with a relatively thick degenerate interface sublayer and additionally with non-regularly distributed columns found to have a high conductivity. Some of them can protrude through the entire structure and thus connect to the surface placed contacts. Such a situation exists in HVPE-GaN epitaxial layers grown directly on sapphire and is described in detail in our earlier works.[19,20] We consider this defective columnar interface region as a quasicontinuous sublayer with a thickness of about 4 μm as can be seen in a panchromatic CL image in cross section of the sample [Fig. 5(a)]. The rest part of the layer is of lower conductivity since the spatial resolved CL spectra taken in that region show a distinguished exciton character. We are aiming to estimate the electrical parameters (n_2 and μ_2) of this region using the extended two-layer model.

The underlying sublayer of such a structure should be considered as completely connected directly to the surface via a conducting column. The case where bypassing vertical columns (rectangulars shown by dashed lines) connect the underlying layer to the contacts is schematically shown in Fig. 5(b). There are two possibilities for connecting the upper layer either through barrier resistances due to a depletion region around the conducting column or through contact resistances directly to the top surface contacts,[6] since a difference between the specific contact resistances connecting the highly conductive column and the surrounding undoped layer can exist. Both connections [Fig. 5(b)] lead to the same conclusion that the upper sublayer can be considered as partially connected, as shown in the equivalent circuit [Fig. 5(c)].

Equations (19) and (20) written for this particular case enable an estimation of the correction factor for the upper layer t_2. For the calculations we use the Hall effect measured value of $n^* = 1.25\times10^{19}$ cm^{-3} and $\mu^* = 66$ cm^2/V s of the whole sample and also the carrier concentration $n_1 = 2.7\times10^{19}$ cm^{-3} of the underlying quasisublayer estimated by calibration procedures of Raman spectra and CL spectra previously reported elsewhere.[17–21]

The estimated value of the correction factor for this sample at the abovementioned fixed parameters n^*, μ^*, and n_1 is about 0.1. This significant correction is expected since the series resistance connecting the upper layer might be significantly large. Using this correction factor we calculate the electrical parameters n_2 and μ_2 which differ noticeably from the measured values for the whole structure. On the other hand, the Hall effect measured parameters of the whole structure are very close to that estimated (by RS and CL) for the underlying sublayer which can be explained considering the underlying sublayer as directly (bypassing) connected to the contacts. Thus, this sublayer will dominate the measured electrical parameters of the whole sample and the contribution of the conductivity and mobility of the upper layer will be underestimated.

It is worth nothing that the conventional two-layer model is nonapplicable to this case. If we directly apply the model using the measured parameters, the calculated values (listed also in Table I) for the upper sublayer will almost coincide with the values of the underlying layer (or to the measured values of the whole structure). However, this is inconsistent with the results obtained from all emission studies.

V. CONCLUSIONS

We have developed a multilayer model for analysis of Hall effect data of samples with top surface contacts and different thicknesses of the sublayers. For this, a detailed balance of the partial layer contribution to the whole sample conductivity and Hall mobility is considered. Circuit analysis is performed accounting for the fact that the sample sublay-

ers are considered as partially connected in parallel to each other by series resistances formed in areas lying below the contacts from each upper layer. Correction factors, which reduce the contribution of the underlying layers to the measured whole sample conductivity, are obtained from the equations relevant to the respective equivalent circuits. A procedure for analysis of the Hall effect data is proposed.

The model is applied for two-layer structures composed of a MOCVD-GaN template layer and HVPE-GaN layer, deposited on a sapphire substrate. The electrical parameters of the templates are independently measured. The electron concentration and mobility of the overgrown HVPE-GaN layers are determined for different structures with different combinations of thicknesses and conductivities of the sublayers and thus, specific approximations of the developed model are demonstrated.

[1] R. L. Petritz, Phys. Rev. **110**, 1254 (1958).

[2] Z. Dziuba, Phys. Status Solidi A **153**, 445 (1996).

[3] Z.-M. Li, S. P. McAlister, and C. M. Hurd, J. Appl. Phys. **66**, 1500 (1989).

[4] E. F. Schubert, K. Ploog, H. Dambkes, and K. Heime, Appl. Phys. A: Solids Surf. **33**, 63 (1984).

[5] S. E. Schacham, R. A. Mena, E. J. Haugland, and S. A. Alterovitz, Appl. Phys. Lett. **62**, 1283 (1993).

[6] C. M. Hurd, S. P. McAlister, W. R. McKinnon, B. R. Stewart, D. J. Day, P. Mandeville, and A. J. SpringThorpe, J. Appl. Phys. **63**, 4706 (1988).

[7] M. J. Kane, N. Apsley, D. A. Anderson, L. L. Taylor, and T. Kerr, J. Phys. C **18**, 5629 (1985).

[8] G. Gregoris, J. Beerens, S. Ben Amor, L. Dmowski, J. C. Portal, D. L. Sivco, and A. Y. Cho, J. Phys. C **20**, 425 (1987).

[9] D. C. Look, *Electrical Characterization of GaAs Materials and Devices* (Wiley, New York, 1989).

[10] D. C. Look, C. E. Stutz, and C. A. Bozada, J. Appl. Phys. **74**, 311 (1993).

[11] W. Gotz, J. Walker, L. T. Romano, N. M. Johnson, and R. J. Molnar, in *III-V Nitrides*, Mater. Res. Soc. Symp. Proc. No. **449**, edited by F. A. Ponce *et al.* (Materials Research Society, Warrendate, PA, 1997) p. 525.

[12] D. C. Look, and R. J. Molnar, Appl. Phys. Lett. **70**, 3377 (1997).

[13] W. Götz, L. T. Romano, J. Walker, N. M. Johnson, and R. J. Molnar, Appl. Phys. Lett. **72**, 1214 (1998).

[14] C. Mavroidis, J. J. Harris, R. B. Jackman, I. Harison, B. J. Ansell, Z. Bougriousa, and I. Moerman, J. Appl. Phys. **91**, 9835 (2002).

[15] L. J. van der Pauw, Philips Res. Rep. **13**, 1 (1958).

[16] J. S. Kim, D. G. Seiler, and W. F. Tseng, J. Appl. Phys. **73**, 8324 (1993).

[17] T. Paskova, S. Tungasmita, E. Valcheva, E. B. Svedberg, B. Arnaudov, S. Evtimova, P. Å. Persson, A. Henry, R. Beccard, M. Heuken, and B. Monemar, MRS Internet J. Nitride Semicond. Res. **5S1**, W.3.14 (2000).

[18] E. Valcheva, T. Paskova, M. V. Abrashev, P. P. Paskov, P. O. Å. Persson, E. M. Goldys, R. Beccard, M. Heuken, and B. Monemar, J. Appl. Phys. **90**, 6011 (2001).

[19] E. M. Goldys, T. Paskova, I. G. Ivanov, B. Arnaudov, and B. Monemar, Appl. Phys. Lett. **73**, 3583 (1998).

[20] B. Arnaudov, T. Paskova, E. M. Goldys, R. Yakimova, Ṡ. Evtimova, I. G. Ivanov, A. Henry, and B. Monemar, J. Appl. Phys. **85**, 7888 (1999).

[21] B. Arnaudov, T. Paskova, E. M. Goldys, S. Evtimova, and B. Monemar, Phys. Rev. B **64**, 045213 (2001).